Calibration of Capacitance Probe Sensors in a Saline Silty Clay Soil

T. J. Kelleners,* R. W. O. Soppe, J. E. Ayars, and T. H. Skaggs

ABSTRACT

Capacitance probe sensors are a popular electromagnetic method of measuring soil water content. However, there is concern about the influence of soil salinity on the sensor readings. In this study capacitance sensors are calibrated for a saline silty clay soil. An electric circuit model is used to relate the sensor's resonant frequency *F* to the permittivity (ε) of the soil. The circuit model is able to account for the effect of dielectric losses on the resonant frequency. Dielectric mixing models and empirical models are used to relate the permittivity to the soil water content (θ). The results show that the electric circuit model does not fit the *F*–ε(θ) data if the calibrated bulk electrical conductivity (EC) model is used. The dielectric losses are overestimated. Increasing the exponent *c* in the tortuosity factor of the bulk EC model and thereby lowering the bulk EC and the dielectric losses improves the performance of the model. Measured and calculated volumetric water contents compare reasonably well (R^2 = 0.884). However, only 73 out of 88 data points can be described. The rejected points are invariably at high water contents where the high dielectric losses result in the sensor frequency being insensitive to ε(θ).

Capacitance probe sensors are a popular electromagnetic method for estimating soil water content (Gardner et al., 2000). The basic principle is to incorporate the soil into an oscillator circuit and measure the resonant frequency. Capacitance probes are relatively cheap, safe, easy to operate, and easily automated. Furthermore, the sensor geometry is very adaptable, facilitating the development of a variety of configurations (Robinson et al., 1998). However, the sensors require a soil specific calibration. And there is concern about the influence of soil salinity and soil temperature on the sensor readings.

Capacitance probe calibrations have been done in the laboratory using packed soil columns (Mead et al., 1995; Paltineanu and Starr, 1997; Baumhardt et al., 2000) and in the field (Bell et al., 1987; Evett and Steiner, 1995; Morgan et al., 1999). All of these calibration studies have directly related the sensor frequency (either scaled or unscaled) to the soil water content. However, the sensors actually react to the capacitance of the soil and access tube system, which, when related to the permittivity of the soil, is a function of the soil water content. Therefore, a more physically consistent calibration procedure involves splitting the calibration into two stages, one in which frequency is related to permittivity, and one in which permittivity is related to soil water content (Robinson et al., 1998; Robinson, 2001).

An advantage of the two-stage approach is that existing dielectric mixing models (e.g., Birchak et al., 1974; Dobson et al., 1985; Friedman, 1998) or empirical models (e.g., Topp et al., 1980; Malicki et al., 1996) can be used to describe the relationship between permittivity and soil water content. The relationship between frequency and permittivity, on the other hand, can be described with electric circuit theory as shown by Dean (1994) and Robinson et al. (1998). Electric circuit theory also makes it possible to account for ionic conductivity effects on the sensor frequency reading.

For the sensors used in this study (EnviroSCAN, Sentek Pty Ltd., Kent Town, South Australia), the appropriate electric circuit model was worked out recently (Kelleners et al., 2004). In that study, the circuit model was calibrated successfully using media (air and fluids) with a wide range of permittivities. The circuit model's ability to describe the effect of ionic conductivity on the sensor's frequency response was confirmed by mixing salts in some of the fluids.

In the current study, EnviroSCAN capacitance probe sensors are calibrated in a saline silty clay soil under field conditions (electrical conductivity of the saturated paste extract [EC_e] ranging from about 6 to 35 dS m^{-1}). The soil water content is related to the sensor's frequency reading by combining the electric circuit model of Kelleners et al. (2004) with the dielectric model of Malicki et al. (1996). More specifically, the objectives are (i) to demonstrate the effect of bulk soil salinity on the sensor frequency, (ii) to test the ability of existing dielectric models to describe the water content–permittivity relationship for the silty clay soil, and (iii) develop a procedure to estimate the soil water content from the sensor frequency using a priori knowledge of the soil salinity.

THEORY

Volumetric Water Content–Permittivity Relationship

The most commonly used empirical equation to relate volumetric water content θ (-) to the relative permittivity ε (-) is that of Topp et al. (1980):

$$\varepsilon = 3.03 + 9.3\theta + 146.0\theta^2 - 76.7\theta^3 \qquad [1]$$

Equation [1] is supposed to hold for mineral soils. Malicki et al. (1996) proposed an alternative empirical equation that covers both organic and mineral soils by taking into account the volume fraction of solid matter (ρ_b/ρ_s) in the soil (where ρ_b is the dry bulk density [M L^{-3}] and ρ_s is the solid phase

T.J. Kelleners and T.H. Skaggs, USDA-ARS, George E. Brown, Jr. Salinity Lab., 450 W. Big Springs Rd., Riverside, CA 92507; T.J. Kelleners, R.W.O. Soppe, and J.E. Ayers, USDA-ARS, Water Management Res. Lab., 9611 S. Riverbend Ave., Parlier, CA 93648; R.W.O. Soppe, currently at Alterra-ILRI, P.O. Box 47, 6700 AA Wageningen, The Netherlands. The mention of trade or manufacturer names is made for information only and does not imply an endorsement, recommendation, or exclusion by the USDA-ARS. Received 28 Aug. 2003. *Corresponding author (tkelleners@ussl.ars.usda.gov).

Published in Soil Sci. Soc. Am. J. 68:770–778 (2004).

677 S. Segoe Rd., Madison, WI 53711 USA

Abbreviations: CEC, cation exchange capacity; EC, electrical conductivity; EC_e, electrical conductivity of the saturated paste extract; SF, scaled frequency; SP, saturation percentage.

density [M L^{-3}]). Written in terms of porosity ϕ (= 1 − ρ_b/ρ_s) (-), their equation reads:

$$\varepsilon = [3.47 - 6.22\phi + 3.82\phi^2 + \theta(7.01 + 6.89\phi - 7.83\phi^2)]^2 \quad [2]$$

Numerous physical and semi-physical dielectric models exist in the literature (see for example Sihvola, 1999). A simple dielectric model that describes the soil as a mixture of solids, water, and air is given by (e.g., Birchak et al., 1974; Roth et al., 1990):

$$\varepsilon = [(1 - \phi)\varepsilon_s^\alpha + \theta\varepsilon_w^\alpha + (\phi - \theta)\varepsilon_a^\alpha]^{1/\alpha} \quad [3]$$

where ε_s, ε_w, and ε_a are the relative permittivities (-) for solids, water and air, respectively. The boundaries for the exponent α in Eq. [3] are −1 and 1, corresponding to three phases in series ($\alpha = -1$) and three phases in parallel ($\alpha = 1$).

Dobson et al. (1985) proposed a popular model based on the work of De Loor (1968) that appears to work well for fine-textured soils (Dirksen and Dasberg, 1993). In this model the soil solids are considered the host medium for randomly distributed and oriented disk-shaped inclusions of the other phases, giving:

$$\varepsilon = \frac{3\varepsilon_s + 2(\theta - \theta_{bw})(\varepsilon_{fw} - \varepsilon_s) + 2\theta_{bw}(\varepsilon_{bw} - \varepsilon_s) + 2(\phi - \theta)(\varepsilon_a - \varepsilon_s)}{3 + (\theta - \theta_{bw})\left(\frac{\varepsilon_s}{\varepsilon_{fw}} - 1\right) + \theta_{bw}\left(\frac{\varepsilon_s}{\varepsilon_{bw}} - 1\right) + (\phi - \theta)\left(\frac{\varepsilon_s}{\varepsilon_a} - 1\right)} \quad [4]$$

where the subscripts bw and fw refer to bound water and free water, respectively. Note that for $\theta < \theta_{bw}$ the second terms in both the numerator and the denominator disappear while θ_{bw} in the third terms change into θ (Miyamoto et al., 2003).

More recently, Friedman (1998) presented a three-phase composite sphere model where the inner phase ε_3 is surrounded by the intermediate phase ε_2, which in turn is surrounded by the outer phase ε_1. The model reads:

$$\varepsilon = \varepsilon_1 + \frac{3\varepsilon_1[(\varphi_3 + \varphi_2)(\varepsilon_2 - \varepsilon_1)(2\varepsilon_2 + \varepsilon_3) - \varphi_3(\varepsilon_2 - \varepsilon_3)(2\varepsilon_2 + \varepsilon_1)]}{\left[(2\varepsilon_1 + \varepsilon_2)(2\varepsilon_2 + \varepsilon_3) - \frac{2\varphi_3}{\varphi_3 + \varphi_2}(\varepsilon_2 - \varepsilon_1)(\varepsilon_2 - \varepsilon_3) - (\varphi_3 + \varphi_2)(\varepsilon_2 - \varepsilon_1)(2\varepsilon_2 + \varepsilon_3) + \varphi_3(\varepsilon_2 - \varepsilon_3)(2\varepsilon_2 + \varepsilon_1)\right]} \quad [5]$$

where φ_1, φ_2, and φ_3 denote the volume fractions of the outer, intermediate, and inner phase, respectively. Note that the outer phase represents the continuous phase in the soil with the other phases acting as discontinuities. Friedman (1998) suggested that a dry soil could be modeled by taking solids as the inner phase ($\varphi_3 = 1 - \phi$), water as the intermediate phase ($\varphi_2 = \theta$) and air as the outer phase ($\varphi_1 = \phi - \theta$). He also suggested that a wet soil could be modeled by taking air as the inner phase ($\varphi_3 = \phi - \theta$), solids as the intermediate phase ($\varphi_2 = 1 - \phi$) and water as the outer phase ($\varphi_1 = \theta$).

The permittivity of the soil as a function of water content according to Eq. [1] through [5] is shown in Fig. 1. Standard average values are taken for the relative permittivities of the soil phases ($\varepsilon_a = 1$, $\varepsilon_s = 5$, and $\varepsilon_w = 80$). The porosity ϕ in Eq. [2] through [5] is taken to be 0.5, while the volume fraction of bound water in Eq. [4] is taken to be 0. Equation [3] is plotted for the exponent $\alpha = -1$ (phases in series) and $\alpha = 1$ (phases in parallel). Equation [5] is plotted for the dry soil configuration and for the wet soil configuration as suggested by Friedman (1998). Figure 1 shows that Eq. [1], [2], and [4] fall in between the extremes set by Eq. [3] and [5]. It is clear that the series and parallel configurations in Eq. [3] constitute the outer boundaries for the ε–θ relationship.

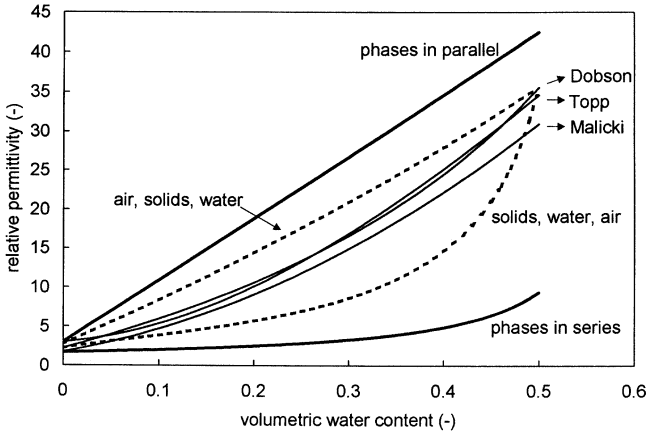

Fig. 1. Relative permittivity as a function of volumetric water content for the empirical models of Topp et al. (1980) and Malicki et al. (1996), and the dielectric mixing models of Dobson et al. (1985), Birchak et al. (1974) (phases in series and in parallel), and Friedman (1998) (solids, water, air configuration and air, solids, water configuration).

Permittivity–Frequency Relationship

The permittivity of the soil can be determined by measuring the soil capacitance:

$$C = g\varepsilon\varepsilon_0 \quad [6]$$

where C is the capacitance ($L^{-2}\,T^4\,M^{-1}\,I^2$), expressed in Farad, g is a geometric factor (L) associated with the electric field penetrating the measured media, and ε_0 (= 8.8542×10^{-12} F m^{-1}) is the permittivity of free space ($L^{-3}\,T^4\,M^{-1}\,I^2$).

A method of measuring the capacitance of the soil is to incorporate it into an oscillator circuit and measure the resonant frequency:

$$F = \frac{1}{2\pi\sqrt{LC_t}} \quad [7]$$

where F is the resonant frequency (T^{-1}) expressed in Hertz, L the total circuit inductance ($L^2\,T^{-2}\,M\,I^{-2}$) expressed in Henry, and C_t the total circuit capacitance.

We assume that the total circuit capacitance for the capacitance probe sensors used in this study is made up of three components, which act both in parallel and in series (Kelleners et al., 2004):

$$C_t = C_s + \frac{C_p C}{C_p + C} \quad [8]$$

where C (= $g_m\varepsilon_m\varepsilon_0$) is the capacitance of the medium, C_p (= $g_p\varepsilon_p\varepsilon_0$) is the capacitance of the plastic access tube surrounding the sensor, and C_s is the capacitance due to stray electric fields. The subscript m denotes the medium and the subscript p denotes the plastic access tube.

Inserting Eq. [8] into Eq. [7] results in:

$$F = \frac{1}{2\pi\sqrt{L\left(C_s + \frac{C_p C}{C_p + C}\right)}} \quad [9]$$

Equation [9] is valid for pure dielectrics. In soil, ionic conduc-

tivity and dielectric relaxation may result in a lossy dielectric. The sum of these losses can be expressed as (after Kraus, 1984):

$$G = g_m\sigma + g_m\omega\varepsilon_{rel}'' \quad [10]$$

where G ($L^{-2}\ T^3\ M^{-1}\ I^2$) is the sum of the losses due to ionic conductivity and relaxation, expressed in Siemens, σ is the bulk EC ($L^{-3}\ T^3\ M^{-1}\ I^2$), expressed in Siemens m^{-1}, ω is the angular frequency (T^{-1}) ($= 2\pi F$) and ε_{rel}'' is the loss factor ($L^{-3}\ T^4\ M^{-1}\ I^2$) due to relaxation expressed in F m^{-1}.

Equation [10] can be incorporated into an expression that describes the resonant frequency of the capacitance probe sensor in lossy dielectrics. The procedure is explained in Kelleners et al. (2004) and is not repeated here. The resulting equation reads:

$$\omega^2 C_A^2 + G^2 - \omega^4 C_s L C_A^2 - \omega^2 C_s L G^2 - \omega^4 L C_p C C_A - \omega^2 L C_p G^2 = 0 \quad [11]$$

where $C_A = C_p + C$. Equation [11] can be solved for the angular frequency ω or for the medium capacitance C using the quadratic formula. Solving for angular frequency requires that G be estimated directly. The G term cannot be calculated analytically using $G = g_m\sigma + g_m\omega\varepsilon_{rel}''$ because ω is not known a priori. On the other hand, when solving for medium capacitance, it should be realized that C is also included in C_A. Application of the quadratic formula to solve for C therefore requires some additional but straightforward algebraic operations. The resulting equations are given in Kelleners et al. (2004).

Expression for Bulk Soil Electrical Conductivity

Working on clay gels, Cremers et al. (1966) used the following relationship to relate bulk EC to the conductivity of the liquid phase and to the surface conductance of the clay:

$$\sigma = \frac{\sigma_w}{f} + \sigma_s' \quad [12]$$

where σ_w is the liquid phase conductivity ($L^{-3}\ M^{-1}\ T^3\ I^2$), σ_s' is the apparent surface conductivity ($L^{-3}\ M^{-1}\ T^3\ I^2$) and f (-) is the formation factor which is a measure of the tortuosity of the porous medium.

Assuming that the bulk soil EC is made up of a liquid phase component and a solid phase component, which act in parallel, Rhoades et al. (1976) gave the following expression for σ:

$$\sigma = \theta\tau\sigma_w + \sigma_s' \quad [13]$$

where τ is a tortuosity factor (-). Equation [13] can be used to describe the EC in unsaturated soil. Note that under saturated conditions Eq. [12] and [13] are equivalent with the convention that $1/f = \theta\tau$ (Shainberg et al., 1980).

In clay-water systems the solid particles are nonconductive. Solid conductivity is due to the ions, which reside in the diffuse double layer. Water in soil is generally situated around or along the solids. Any separation between the ions in the diffuse double layer and the ions in the pore water is therefore arbitrary. It is therefore reasonable to assume that the same formation factor f applies for the liquid phase conductivity and the surface conductivity. Thus, Eq. [12] can also be written as (Cremers and Laudelout, 1965; Shainberg et al., 1980; Nadler and Frenkel, 1980):

$$\sigma = \frac{\sigma_w}{f} + \delta\frac{\sigma_s}{f} \quad [14]$$

where σ_s is the surface conductivity ($L^{-3}\ M^{-1}\ T^3\ I^2$) due to the cations in the diffuse double layer. The empirical factor δ (-) is included in Eq. [14] to describe the reduction in σ_s/f with σ_w when σ_w falls below a certain threshold value (usually between 1 and 4 dS m^{-1}). This reduction, which is commonly observed during laboratory experiments, could be the result of ions in the diffuse double layer being isolated from each other by patches of low conductivity solution (Bolt, 1979). In a similar way, Eq. [13] can be written as (Nadler and Frenkel, 1980; Jurinak et al., 1987):

$$\sigma = \theta\tau\sigma_w + \delta\theta\tau\sigma_s \quad [15]$$

Equation [15] is better suited to describe the EC in soil over a wide range of moisture contents than Eq. [13], which was developed primarily to relate bulk soil EC to the EC of the soil water for soils near field capacity. For low water contents, σ in Eq. [15] may approach 0, which is more realistic than the lower limit of $\sigma = \sigma_s'$ in Eq. [13]. It should be noted that Eq. [15] no longer assumes that σ is the sum of two phases in parallel. Instead σ_w and σ_s now relate to the same volume fraction $\theta\tau$, and a supposedly continuous distribution of conductivities is replaced by two values, the reference value for the soil water and the space average of the excess conductance (e.g., Cremers et al., 1966).

Several forms of the tortuosity factor τ were reviewed by Amente et al. (2000). In this study two formulations are tested:

$$\tau = a\theta + b \quad [16]$$

which was proposed by Rhoades et al. (1976) and:

$$\tau = (\theta - \theta_0)^c \quad [17]$$

which is derived from a model that describes gas diffusion in soil (Marshall, 1959; Amente et al., 2000). In Eq. [16] and [17], a, b, and c are empirical coefficients (-) and θ_0 is the portion of the volumetric water content (-) that is close to the solid particles where ions are considered immobile.

MATERIALS AND METHODS

The capacitance probe calibration was conducted at an abandoned agricultural field plot about 8 km southwest of the town of Tranquillity in California's San Joaquin Valley. At the time of the experiment, the plot was overgrown with natural grass. The soil is a saline silty clay (fine, smectitic, thermic, sodic Haploxerert), which was mapped as Oxalis series in the original soil survey in 1940. A detailed description of the soil profile is given in Table 1. The soil was compacted between the 20- and 40-cm depths, presumably due to past tillage traffic. The field work was conducted between 29 Mar. and 13 June 2002. During this time the groundwater table was not observed

Table 1. Selected physical and chemical data for the studied soil.

Horizon	Depth	Sand	Silt	Clay	Class	ρ_b	EC_e	SAR†	SP
	cm		%			g cm^{-3}	dS m^{-1}	$(mmol_c\ L^{-1})^{1/2}$	
Ap	0–20	6.0	43.6	50.4	silty clay	1.11	9.0	7.9	61.9
B1	20–75	2.6	43.9	53.5	silty clay	1.38	28.4	60.9	73.5
B2	75–120	4.6	27.5	67.9	clay	1.32	28.0	65.8	82.4

† Sodium adsorption ratio defined as $Na^+/\sqrt{(\frac{1}{2}Ca^{2+} + \frac{1}{2}Mg^{2+})}$ (concentration in $mmol_c\ L^{-1}$).

within 270 cm of the soil surface. Rainfall during this period was small (8.3 mm according to the Westlands weather station, located 2.5 km to the west).

Three polyvinyl chloride (PVC) capacitance probe access tubes were installed to a depth of about 120 cm below the soil surface using a hydraulic soil-drilling machine mounted on a rig (Giddings Machine Company, Ft. Collins, CO). One access tube (Location B) was later disregarded because of suspected air gaps between the tube wall and the surrounding soil. Two EnviroSCAN capacitance probes were used. Probe 1 held 14 sensors while Probe 2 held 15 sensors (one sensor on Probe 1 was damaged during the field work). The vertical spacing between the sensors was 10 cm. Detailed information about the EnviroSCAN sensor can be found in Paltineanu and Starr (1997). On 29 Mar. and 4 June 2002, both probes were inserted in the first access tube (designated Location A) and the sensor frequencies were recorded. Because some of the sensors were located above soil surface, only 23 out of 29 sensors gave a meaningful reading. Similarly, on 5 Apr. and 13 June 2002, both probes were inserted in the other access tube (Location C) and the sensor frequencies were recorded. For Location C, 21 sensors gave a meaningful reading.

On each of the four experimental dates a pit was dug close to the relevant access tube and two soil samples were taken at each sensor depth. In the first pit at each location, the sampling was done far enough away from the access tube to avoid impacting the sensor readings on the second experimental date. The sampling was done about 15 cm away from the access tube wall, which is about equal to the radial sensitivity of the EnviroSCAN sensors (Paltineanu and Starr, 1997). The pit was carefully backfilled after the first sampling. The second pit at each location was dug on the opposite side of the access tube. The cylindrical soil samples (diameter 5.4 cm; height 6 cm) were analyzed in the laboratory for gravimetric water content, saturation percentage (SP), EC_e, pH, ion composition, and soil texture using standard procedures.

In addition, on 4 June 2002 (Location A) and on 13 June 2002 (Location C), bulk soil EC ($= \sigma$) was measured at the sensor depths using a horizontally inserted four electrode probe connected to a combination electrical generator and resistance meter (SCT meter, Martek Instruments, Inc., Raleigh, NC). Soil temperature was measured at the same depths using a horizontally inserted thermometer. The bulk soil EC at a 25°C reference temperature was calculated using $\sigma(25) = \sigma(T) - 0.02\sigma(T)(T - 25)$ (Jurinak and Suarez, 1990), where T is the measured soil temperature in degrees Celsius.

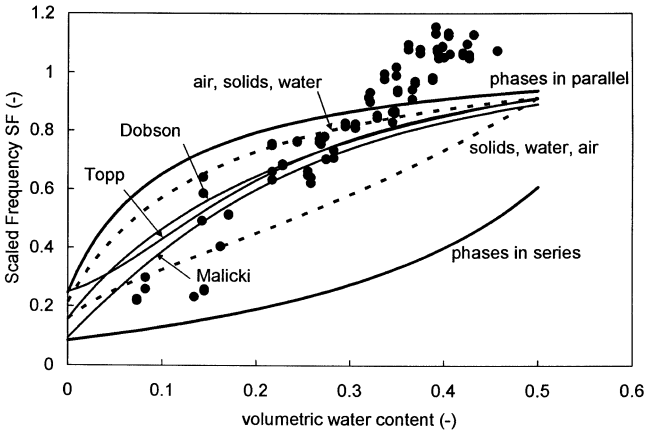

Fig. 2. Scaled frequency as a function of volumetric water content as measured in the field (dots) and as calculated by combining the circuit model for nonlossy media with five models that describe the relative permittivity as a function of soil water content (lines). The model of Birchak et al. (1974) is given for phases in series and for phases in parallel. The model of Friedman (1998) is given for the solids, water, air configuration, and the air, solids, water configuration.

RESULTS AND DISCUSSION

Volumetric Water Content versus Scaled Frequency

The relationship between volumetric water content and sensor frequency is visualized in Fig. 2 by plotting the volumetric water content against the scaled frequency, SF (-):

$$\mathrm{SF} = \frac{F_a - F_s}{F_a - F_w} \qquad [18]$$

where F_a is the sensor frequency (T^{-1}) in air, F_s the sensor frequency (T^{-1}) in soil, and F_w the sensor frequency (T^{-1}) in deionized water.

The sensor frequency values are scaled because not all sensors behave exactly the same. The scaling procedure is explained in more detail in Paltineanu and Starr (1997). The air and water frequencies for the sensors used in the present study were taken from Kelleners et al. (2004).

Figure 2 shows the measured data for all eight combinations of the four sampling dates and the two capacitance probes. The curves in Fig. 2 are calculated by combining the theoretical frequency response in nonlossy media (Eq. [9]) with the five permittivity–water content relationships presented in the theory section (Eq. [1]–[5]). For Eq. [3] and [5] again the two extremes are shown (phases in series and in parallel, and the dry soil and wet soil configurations, respectively). Input parameters for Eq. [1] to [5] are the same as for Fig. 1. In addition the relative permittivity of the plastic access tube is assumed to be 3 (e.g., Von Hippel, 1954). All curves are for the tenth sensor on Probe 1. The required sensor constants ($C_s = 10.41 \times 10^{-12}$ F, $L = 9.38 \times 10^{-8}$ H, $g_m = 0.174$ m and $g_p = 0.619$ m) are taken from Table 1 in Kelleners et al. (2004). Calculated curves for all other sensors are very similar and are therefore not shown.

Note that all curves in Fig. 2, except the one based on Eq. [1], are influenced by the value of porosity. The selected value of $\phi = 0.5$ is the approximate median value for the measured data (range 0.40 to 0.63). In addition, the curve based on Eq. [4] is also sensitive to the volume fraction of bound water. A value of $\theta_{bw} = 0$ is selected to allow a fair comparison with the other ε–θ relationships. As a consequence, Fig. 2 should not be used to judge which ε–θ relationship performs best for our data. Instead, the figure is intended to show how the field data compare with existing dielectric models under the assumption that there are no dielectric losses.

Figure 2 shows that for $\theta < 0.31$ the data fall in between the extremes set by the curves that represent the phases in series and phases in parallel. Furthermore most data with $\theta < 0.31$ fall in between the extremes set for the dry and wet soil. In contrast, for $\theta > 0.31$,

many data points have SF values that exceed the ones predicted by the phases in parallel model. Also many data points have SF values higher than 1. If SF > 1, than $F_s < F_w$ (Eq. [18]), which would be improbable in a nonlossy soil. The most likely explanation is that for $\theta > 0.31$ the dielectric losses due to ionic conductivity and/or relaxation start to have a significant impact on the sensor's frequency reading in soil. The higher the dielectric losses, the lower F_s, and the higher SF. Varying the value of porosity for the calculated curves does not change this observation (results not shown).

Calibration of the Bulk Soil Electrical Conductivity Model

Equation [15] is used in combination with Eq. [16] and [17] to describe the bulk EC (σ) of the soil as a function of σ_w and σ_s. Values of σ_w are derived in two different ways. First, σ_w is calculated from the EC_e ($= \sigma_e$) by $\sigma_w = (\rho_b/\rho_w)(SP/100)(\sigma_e/\theta)$, where ρ_w is the density of water. This assumes that precipitation/dissolution of salts due to changes in soil water content can be neglected. Second, σ_w is calculated from the ion composition using the PHREEQC model (Parkhurst and Appelo, 1999), which accounts for precipitation/dissolution processes due to variations in the water content. The PHREEQC results show that significant amounts of $CaSO_4$ and $MgSO_4$ precipitate/dissolve with changing water content in this saline soil where sulfate is the dominant anion. As a result, the σ_w values calculated by the first method (varying between 28.6 and 159.0 dS m^{-1}) are consistently higher than the σ_w values calculated by the second method (varying between 21.0 and 134.0 dS m^{-1}). In view of these results, we only use the lower σ_w values calculated with PHREEQC in the subsequent analysis.

The surface conductance (σ_s) is calculated by (e.g., Nadler and Frenkel, 1980):

$$\sigma_s = \frac{\lambda^e_{cat}\rho_s CEC}{\theta} \qquad [19]$$

where λ^e_{cat} is the effective equivalent ionic conductivity of the exchangeable cations (S m^2 $mmol_c^{-1}$) and CEC is the cation exchange capacity of the soil (mol_c g^{-1} of soil).

The value of λ^e_{cat} depends on the type of cation on the exchange complex. For each cation, the exact value depends on the equivalent ionic conductivity of the cation in an aqueous solution at infinite dilution (λ^0_{cat}) and a correction factor (ζ) accounting for the reduction in ion mobility near surfaces. The mobility of cations near solids is reduced due to electrical interaction and due to a reduction in the fluidity of water (Shainberg and Kemper, 1966). At this time there is not enough information available to calculate λ^e_{cat} for a mixture of cations. As a first approximation, λ^e_{cat} is calculated by assuming that the dominant cation in the soil solution occupies all exchange sites. At all four soil pits, Ca^{2+} is the dominant cation in the topsoil ($\lambda^e_{cat} = \zeta\lambda^0_{Ca} = 0.06 \times 59.5$ S cm^2 mol_c^{-1} at 0- to 20-cm depth). Below 20 cm, Na^+ is the dominant cation ($\lambda^e_{cat} = \zeta\lambda^0_{Na} = 0.40 \times 50.1$ S cm^2 mol_c^{-1}). Values for λ^0_{cat} are taken from Weast (1985). The values for ζ are estimated from EC measurements on clay gels and soils conducted by Shainberg and coworkers (Shainberg and Kemper, 1966; Shainberg and Levy, 1975; Shainberg et al., 1980; Shainberg et al., 1982).

The CEC of the silty clay soil was measured previously by the USDA on samples from a similar soil taken at a location about 2.5 km northwest of our site (Pedon No. 85P0986, Soil Survey Staff, 2003). The CEC between the 0- and 152-cm depth ranged between 32.5 and 38.1 $mmol_c$ per 100 g of soil. For this study we take an average value of 36.3 $mmol_c$ per 100 g, which is assumed to be constant with depth. For the solid phase density ρ_s we assume a value of 2.65 g cm^{-3}. The calculated values for σ_s (Eq. [19]) range between 20.2 and 89.0 dS m^{-1}. Note that σ_w and σ_s have the same order of magnitude. Finally, because of the high values of σ_w, it is safe to assume that $\delta = 1$ in Eq. [15] (e.g., Nadler and Frenkel, 1980).

The parameters in the two tortuosity models (Eq. [16] and [17]) are obtained by fitting Eq. [15] to the measured σ values. For Eq. [16] this results in $a = 1.512$ and $b = -0.258$ ($R^2 = 0.920$). For Eq. [17] this results in $\theta_0 = 0.245$ and $c = 0.555$ ($R^2 = 0.934$). The comparison between the measured and calculated bulk EC of the soil at a reference temperature of 25°C is shown in Fig. 3. The figure and the R^2 values show that Eq. [17] gives slightly better results than Eq. [16]. This is an unexpected outcome. Previous studies have shown that Eq. [16] is suitable for describing tortuosity in clayey soils (e.g., Rhoades et al., 1976) while Eq. [17] is suitable for describing tortuosity in sandy soils (e.g., Amente et al., 2000). The θ_0 value in Eq. [17] indicates that for water contents below 0.245 there is no significant EC in the soil. For Eq. [16] a similar threshold value can be calculated by noting that $\tau = 0$ if $\theta = -b/a$ (Rhoades et al., 1976). The resulting threshold water content is 0.171.

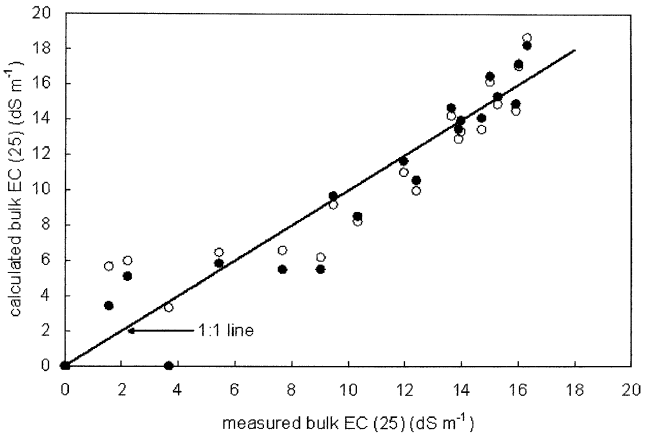

Fig. 3. Measured versus calculated bulk electrical conductivity (EC) at 25°C using the tortuosity factor of Rhoades et al. (1976) (Eq. [16], open circles) and using the tortuosity factor derived from the gas diffusion model of Marshall (1959) (Eq. [17], filled circles).

Application of the Electric Circuit Model

The electric circuit model developed by Kelleners et al. (2004) (Eq. [11] in the current paper) should be able to describe the measured frequency response in the soil. The model can only be applied if the dielectric losses G in the soil are known. Unfortunately, the losses due to relaxation are unknown at this time. Therefore, as a first approximation, it is assumed that the dielectric losses are solely due to ionic conductivity. Hence, it is assumed that $G = g_m\sigma$.

To compare the electric circuit model with the field data we need to select a dielectric model that describes the ε–θ relationship. We opt for the model of Malicki et al. (1996) because it is simple, does not require calibration, takes into account the variations in porosity and fits the data well (judging from the data points in Fig. 2 that are not affected by dielectric losses). The results are shown in Fig. 4 for both tortuosity models (Eq. [16] and [17]). The calculated curves are again only for the tenth sensor on Probe 1, assuming a porosity value of 0.5. Apart from the curve that assumes no dielectric losses, three other curves are shown for each tortuosity model having σ_w values of 30, 60, and 90 dS m^{-1} (measured σ_w values are between 21.0 and 134.0 dS m^{-1}) and a σ_s value of 60 dS m^{-1} (σ_s values estimated from the CEC are between 20.2 and 89.0 dS m^{-1}). Calculated curves for all other sensors are very similar (results not shown). It is stressed that Fig. 4 can only be used for a general comparison between the circuit model and the field data. Each data point has specific values for ϕ, σ_w, and σ_s, and is associated with one particular sensor. Each point therefore requires a separate model calculation.

Figure 4 shows that the circuit model does not fit the data. Note that the water content values at which the calculated curves for σ_w = 30, 60, and 90 dS m^{-1} start to deviate from the no-losses curve coincide with the threshold water contents of 0.171 and 0.245 in the tortuosity models. The bad fit for both tortuosity models seems to show that the dielectric losses G, and therefore σ are overestimated. This indicates that the capacitance sensors experience a different value of σ than that measured by the four-electrode probe. This might be due to (i) differences in electrode configuration and measurement volume, (ii) the orientation of the electromagnetic field (horizontal for the four-electrode probe as opposed to vertical for the capacitance sensors), or (iii) the installation procedure (pushing for the four-electrode probe [soil compaction] versus digging for the capacitance sensors).

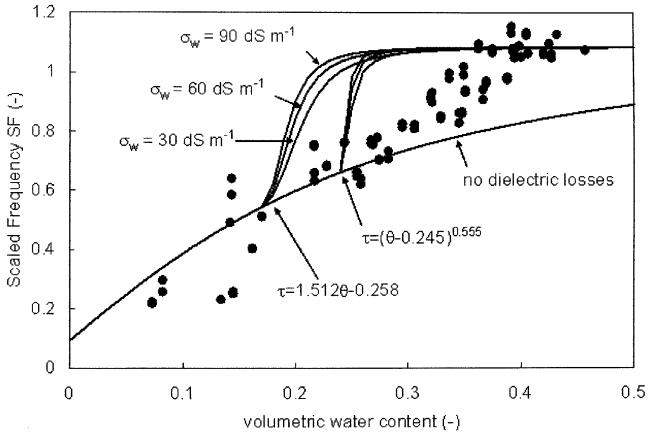

Fig. 4. Scaled frequency as a function of volumetric water content as measured in the field (dots) and as calculated with a combination of the electric circuit model for lossy media and the empirical $\varepsilon(\theta)$ relationship of Malicki et al. (1996) (lines). Calculations assume no dielectric losses and σ_w = 30, 60, and 90 dS m^{-1} combined with σ_s = 60 dS m^{-1}. The tortuosity factor of Rhoades et al. (1976) and the tortuosity factor derived from the gas diffusion model of Marshall (1959) are used to calculate bulk electrical conductivity.

To demonstrate the effect of lower values of σ on the calculated curves without changing the values of σ_w and σ_s, we adjust the exponent c in the tortuosity model as given by Eq. [17]. This adjustment in the model is particularly relevant if the above explanation (ii) is true. If the soil is anisotropic with the solid particles aligned horizontally, the tortuosity in the horizontal direction is likely to be different from the tortuosity in the vertical direction. Figure 5 shows the calculated curves for σ_w = 30, 60, 90 dS m^{-1} and σ_s = 60 dS m^{-1} with c = 1.25. Clearly, the calculated curves now compare much better with the field data. Evidence of electrical anisotropy of clay-like materials was given by Mousseau and Trump (1967) who observed ratios between vertical and horizontal resistivity of 18.2 and 25.5 for Bentonite slurry and 3.9 for Kaolinite slurry. It is likely that the electrical anisotropy is not constant but a function of the soil water content (e.g., Friedman and Jones, 2001).

In the next section the circuit model will be applied to all data points separately, and the optimum value for c will be determined.

Measured versus Calculated Soil Water Content

A FORTRAN program was written to calculate the water content for each individual data point combining the circuit model (Eq. [11]) and the ε–θ relationship of Malicki et al. (1996) (Eq. [2]).

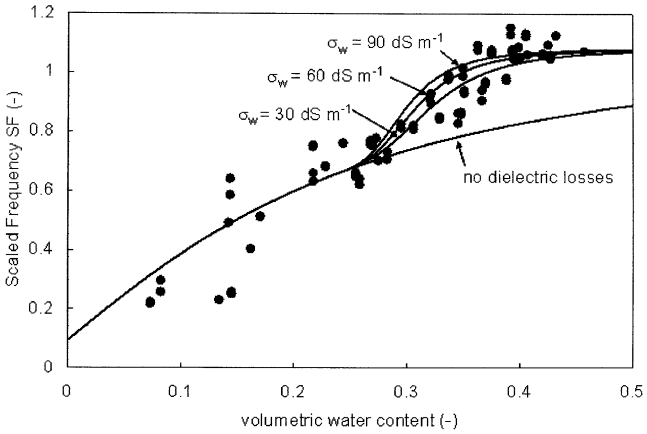

Fig. 5. Scaled frequency as a function of volumetric water content as measured in the field (dots) and as calculated with a combination of the electric circuit model for lossy media and the empirical $\varepsilon(\theta)$ relationship of Malicki et al. (1996) (lines). Calculations assume no dielectric losses and σ_w = 30, 60, and 90 dS m^{-1} combined with σ_s = 60 dS m^{-1}. Exponent c = 1.25 is used in the calculation of the tortuosity factor derived from Marshall (1959).

Table 2. Number of modeled points (No.) and sum of squared differences between measured and calculated volumetric water content (SSQ) as a function of the exponent *c* in Eq. [17].

c	No.	SSQ	SSQ/No.	*c*	No.	SSQ	SSQ/No.
0.1	78	0.662	0.0085	1.06	74	0.125	0.0017
0.2	78	0.647	0.0083	1.07	74	0.122	0.0017
0.3	76	0.629	0.0083	1.08	74	0.120	0.0016
0.4	76	0.589	0.0078	1.09	74	0.118	0.0016
0.5	76	0.522	0.0069	1.10	74	0.116	0.0016
0.6	76	0.438	0.0058	1.11	74	0.114	0.0015
0.7	76	0.348	0.0046	1.12	74	0.112	0.0015
0.8	76	0.267	0.0035	1.13	74	0.111	0.0015
0.9	76	0.200	0.0026	1.14	74	0.110	0.0015
1.0	75	0.148	0.0020	1.15	74	0.109	0.0015
1.1	74	0.116	0.0016	1.16	74	0.108	0.0015
1.2	73	0.100	0.0014	1.17	74	0.107	0.0015
1.3	73	0.109	0.0015	1.18	74	0.108	0.0015
1.4	71	0.120	0.0017	1.19	73	0.100	0.0014
1.5	68	0.121	0.0018	1.20	73	0.100	0.0014
1.6	65	0.121	0.0019	1.21	73	0.099	0.0014
1.7	64	0.142	0.0022	1.22	73	0.100	0.0014
1.8	64	0.179	0.0028	1.23	73	0.100	0.0014
1.9	63	0.202	0.0032	1.24	73	0.101	0.0014
2.0	63	0.245	0.0039	1.25	73	0.102	0.0014
2.1	61	0.258	0.0042	1.26	73	0.103	0.0014
2.2	59	0.257	0.0044	1.27	73	0.104	0.0014
2.3	57	0.251	0.0044	1.28	73	0.105	0.0014
2.4	54	0.229	0.0043	1.29	73	0.107	0.0015
2.5	52	0.204	0.0039	1.30	73	0.109	0.0015
2.6	52	0.216	0.0042	1.31	73	0.111	0.0015
2.7	49	0.170	0.0035	1.32	72	0.108	0.0015
2.8	48	0.154	0.0032	1.33	72	0.110	0.0015
2.9	48	0.156	0.0032	1.34	72	0.112	0.0016
3.0	48	0.157	0.0033	1.35	72	0.115	0.0016

Directly solving for water content would require a numerical method because both the capacitance of the soil C and the dielectric losses G in Eq. [11] are a function of θ. The fact that Eq. [11] may have two positive solutions for C if the frequency F is input, further complicates matters. In this work we therefore reversed the calculation. For each data point the volumetric water content θ is varied between 0.0005 and the porosity using an increment of 0.001. For each value of θ, ε (Eq. [2]), C (Eq. [6]), σ (Eq. [15] and [17]), G ($= g_m\sigma$), F (Eq. [11]), and the difference between the calculated and measured sensor frequency ($= \triangle F$) are calculated. There is a solution if $\triangle F = 0$ or if $\triangle F$ changes sign between two subsequent θ values. In the latter case, the calculation is repeated using the average θ value, which is then taken as the solution. Note that $\theta = 0$ cannot be considered because of the θ value in the denominator of Eq. [19].

To make the approach more generally applicable, we calculated the sensor constants in Eq. [11] with the simplified procedure of Kelleners et al. (2004). In brief, the simplified procedure fixes the sensor constants L at 9.38×10^{-8} H and g_m at 0.176 m. Subsequently, the two remainder sensor constants g_p and C_s are calculated by solving Eq. [9] using sensor readings in air and deionized water. Previously, this procedure resulted in R^2 values between 0.999 and 1.0 when measured and calculated permittivities of eight nonconductive media were compared (see Kelleners et al., 2004).

We ran the FORTRAN program for several values of the exponent c in Eq. [17]. The best value of c is selected on the basis of two criteria: (i) the number of data points that are successfully modeled (i.e., for which a solution is found with Eq. [11]), and (ii) the sum of squared differences between the measured and calculated volumetric water contents. Table 2 shows that the optimum value for c, based on the ratio between the sum of squared differences and the number of points, lays somewhere between 1.19 and 1.28. On the basis of these results we selected $c = 1.21$ (lowest sum of squares). This value of c should be interpreted as an effective parameter for determining the total dielectric losses because of the neglect of the losses due to relaxation mentioned earlier (e.g., Topp et al., 1988). Note that we did not encounter data points with two solutions for θ.

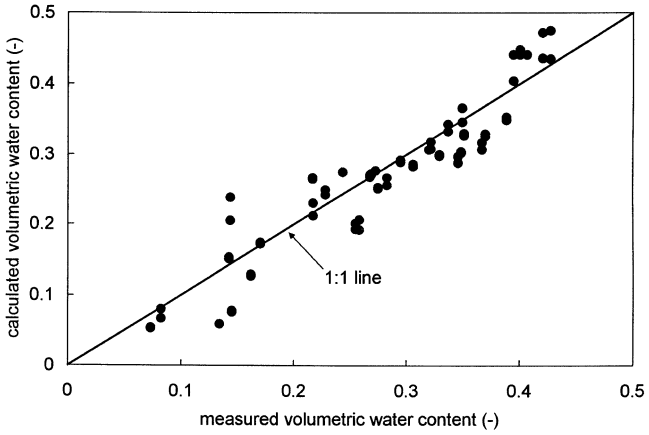

Fig. 6. Measured versus calculated volumetric water content. Calculated values are obtained by combining the circuit model for lossy media with the empirical ε(θ) relationship of Malicki et al. (1996). Exponent $c = 1.21$ is used in the calculation of the tortuosity factor derived from Marshall (1959).

A plot of measured versus calculated volumetric water content for $c = 1.21$ is shown in Fig. 6. The fit is reasonable ($R^2 = 0.884$). Only 73 data points are shown in Fig. 6. The other 15 points did not give a solution. Points without a solution are invariably in the high water content range. At high water contents the dielectric losses G are high and the resonant frequency is insensitive to permittivity and hence to water content. However, even at high water contents there still appears to be a relationship between F and θ (see Fig. 2). This is due to the fact that, in wet saline soils, F is influenced by G, with G being a function of water content. So indirectly there remains some relationship between F and θ at high water contents. Because the direct relationship between F and ε(θ) is lost, however, the consequence of using capacitance sensors in saline soil is that F values in wet soil cannot always be converted into reliable water content values.

The spread in the water content values around the 1:1 line in Fig. 6 is appreciable. Most of the spreading is probably due to the use of an undisturbed field soil, which is heterogeneous and which has a distinct soil structure (especially in the topsoil). The relatively small sampling volume of the capacitance probe sensors, which is a result of the presence of the plastic access tube, makes the sensors susceptible to these small-scale heterogeneities. The soil heterogeneity will also be reflected in the soil samples (two samples for each data point). Finally, the presence of air gaps between the

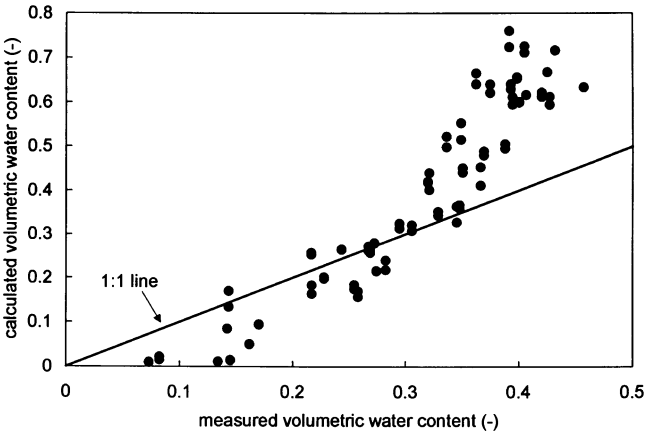

Fig. 7. Measured versus calculated volumetric water content. Calculated values are obtained with the factory calibration for the EnviroSCAN sensors.

access tube and the soil, which develop when the soil dries, may result in the underestimation of some of the calculated water contents.

Finally, the data obtained during this study can be used to check the performance of the factory calibration that comes with the EnviroSCAN sensors. The calibration equation is: $SF = A\ (100\theta)^B + D$, where $A = 0.19570$, $B = 0.40400$, and $D = 0.02852$. Note that in this equation the differences in porosity between sampling depths cannot be taken into account. Also, there is no mechanism to account for the effect of dielectric losses on the resonant frequency. Figure 7 shows the comparison between measured and calculated volumetric water content. It is obvious that the factory calibration does not perform well ($R^2 = 0.879$). At low water contents, θ is underestimated, while at high water contents, θ is overestimated by as much as 80%. Use of the factory calibration therefore leads to large systematic errors for the saline silty clay soil used in this study.

The results of this study show that the electric circuit model of Kelleners et al. (2004) combined with an existing $\varepsilon(\theta)$ relationship is successful in calculating the soil water content from capacitance sensor readings. However, the procedure for our saline silty clay soil requires a lot of information. Calculating the dielectric losses G requires data on tortuosity, EC_e, CEC, ion composition, and ion mobility. Inclusion of the relaxation losses in G would increase the amount of required data even more. It should be pointed out however, that the saline silty clay soil used in this study constitutes a worst-case scenario. Less saline more coarse-textured soils will allow for a more simple procedure. For example, if the dielectric losses can be neglected all together, only sensor frequency readings in air and water are needed to obtain the parameters for relating the sensor frequency F to $\varepsilon(\theta)$.

CONCLUSIONS

Field data from the saline silty clay soil show that the effect of dielectric losses on the capacitance sensors becomes apparent at a volumetric water content (θ) of 0.31 or higher. Below this threshold, the dielectric models of Topp et al. (1980), Dobson et al. (1985), and Malicki et al. (1996) in combination with the circuit model for nonlossy soil all match the data reasonably well. Above this threshold the effect of the dielectric losses G on the sensors' resonant frequency needs to be taken into account.

The bulk EC of the soil was described using two different formulations for the tortuosity factor τ. The tortuosity formulation derived from a gas diffusion model of Marshall (1959) fits the data slightly better than the tortuosity formulation of Rhoades et al. (1976) (R^2 values of 0.934 and 0.920, respectively). The optimized value for the threshold water content in the formulation derived from Marshall's model indicates that below $\theta = 0.245$ the soil is basically nonconductive. In other words, below $\theta = 0.245$, there are no significant continuous pathways in the soil that support an electrical current.

The electric circuit model for lossy materials does not accurately describe the field data if the bulk EC is calculated with the calibrated tortuosity parameters. The frequency readings from the capacitance sensors show that the bulk EC and hence the dielectric losses are overestimated. The circuit model fits the field data much better if the bulk soil EC is lowered by increasing the exponent c in the tortuosity model derived from Marshall (1959). This adjustment is justifiable if the soil is considered anisotropic with tortuosity in the horizontal direction being lower (high τ) than tortuosity in the vertical direction (low τ).

The electric circuit model with an adjusted value for the exponent c of 1.21 in the tortuosity model gives a satisfactory description of the measured F–θ data. Measured and calculated volumetric water contents compare reasonably well ($R^2 = 0.884$). However, only 73 out of 88 data points can be described. The rejected points are invariably at high water contents where the high dielectric losses result in the sensor frequency being insensitive to $\varepsilon(\theta)$. Application of capacitance sensors in saline soil might result in the loss of field data because frequencies in wet soil cannot always be converted into a reliable value for the water content.

ACKNOWLEDGMENTS

The authors thank Renae Muniz, Stephanie Andersen, and Tom Pflaum at USDA-ARS, Parlier for their help during the fieldwork and for the soil analysis in the laboratory, and David Robinson (USDA-ARS, Riverside, CA) for the many stimulating discussions.

REFERENCES

Amente, G., J.M. Baker, and C.F. Reece. 2000. Estimation of soil solution electrical conductivity from bulk soil electrical conductivity in sandy soils. Soil Sci. Soc. Am. J. 64:1931–1939.

Baumhardt, R.L., R.J. Lascano, and S.R. Evett. 2000. Soil material, temperature, and salinity effects on calibration of multisensor capacitance probes. Soil Sci. Soc. Am. J. 64:1940–1946.

Bell, J.P., T.J. Dean, and M.G. Hodnett. 1987. Soil moisture measurement by an improved capacitance technique. Part II. Field techniques, evaluation and calibration. J. Hydrol. (Amsterdam) 93: 79–90.

Birchak, J.R., C.G. Gardner, J.E. Hipp, and J.M. Victor. 1974. High

dielectric constant microwave probes for sensing soil moisture. Proc. IEEE 62:93–98.
Bolt, G.H. 1979. Electrochemical phenomena in soil and clay systems. p. 387–432. *In* G.H. Bolt (ed.) Soil chemistry B. Physico-chemical models. Developments in soil science 5B. Elsevier, Amsterdam, The Netherlands.
Cremers, A., and H. Laudelout. 1965. On the "isoconductivity value" of clay gels. Soil Sci. 100:298–299.
Cremers, A., J. van Loon, and H. Laudelout. 1966. Geometry effects for specific electrical conductance in clays and soils. p. 149–162. *In* Proc. 14th Nat. Conf. Clays and Clay Minerals. Pergamon Press, Oxford, UK.
Dean, T.J. 1994. The IH capacitance probe for measurement of soil water content. Rep. No. 125, Institute of Hydrology, Wallingford, UK.
De Loor, G.P. 1968. Dielectric properties of heterogeneous mixtures containing water. J. Microw. Power 3:67–73.
Dirksen, C., and S. Dasberg. 1993. Improved calibration of time domain reflectometry soil water content measurements. Soil Sci. Soc. Am. J. 57:660–667.
Dobson, M.C., F.T. Ulaby, M.T. Hallikainen, and M.A. El-Rayes. 1985. Microwave dielectric behavior of wet soil. Part II: Dielectric mixing models. IEEE Trans. Geosci. Remote Sens. GE-23:35–46.
Evett, S.R., and J.L. Steiner. 1995. Precision of neutron scattering and capacitance type soil water content gauges from field calibration. Soil Sci. Soc. Am. J. 59:961–968.
Friedman, S.P. 1998. A saturation degree-dependent composite spheres model for describing the effective dielectric constant of unsaturated porous media. Water Resour. Res. 34:2949–2961.
Friedman, S.P., and S.B. Jones. 2001. Measurement and approximate critical path analysis of the pore-scale-induced anisotropy factor of an unsaturated porous medium. Water Resour. Res. 37:2929–2942.
Gardner, C.M.K., D.A. Robinson, K. Blyth, and J.D. Cooper. 2000. Soil water content. p. 1–64. *In* K.A. Smith, and C.E. Mullins (ed.) Soil and environmental analysis: Physical methods. Marcel Dekker, New York.
Jurinak, J.J., S.S. Sandhu, and L.M. Dudley. 1987. Ionic diffusion coefficients as predicted by conductometric techniques. Soil Sci. Soc. Am. J. 51:625–630.
Jurinak, J.J., and D.L. Suarez. 1990. The chemistry of salt-affected soils and waters. p. 42–63. *In* K.K. Tanji (ed.) Agricultural salinity assessment and management. ASCE manuals and reports on engineering practice No. 71. ASCE, New York.
Kelleners, T.J., R.W.O. Soppe, D.A. Robinson, M.G. Schaap, J.E. Ayars, and T.H. Skaggs. 2004 Calibration of capacitance probe sensors using electric circuit theory. Soil Sci. Soc. Am. J. 68:430–439.
Kraus, J.D. 1984. Electromagnetics. 3rd ed. McGraw-Hill.
Malicki, M.A., R. Plagge, and C.H. Roth. 1996. Improving the calibration of dielectric TDR soil moisture determination taking into account the solid soil. Eur. J. Soil Sci. 47:357–366.
Marshall, T.J. 1959. The diffusion of gases through porous media. J. Soil Sci. 10:79–84.
Mead, R.M., J.E. Ayars, and J. Liu. 1995. Evaluating the influence of soil texture, bulk density and soil water salinity on a capacitance probe calibration. ASAE Paper 95–3264. ASAE, St. Joseph, MI.
Miyamoto, T., T. Annaka, and J. Chikushi. 2003. Soil aggregate structure effects on dielectric permittivity of an Andisol measured by time domain reflectometry. Vadose Zone J. 2:90–97.
Morgan, K.T., L.R. Parsons, T.A. Wheaton, D.J. Pitts, and T.A. Obreza. 1999. Field calibration of a capacitance water content probe in fine sand soils. Soil Sci. Soc. Am. J. 63:987–989.
Mousseau, R.J., and R.P. Trump. 1967. Measurement of electrical anisotropy of clay-like materials. J. Appl. Phys. 38:4375–4379.
Nadler, A., and H. Frenkel. 1980. Determination of soil solution electrical conductivity from bulk soil electrical conductivity measurements by the four-electrode method. Soil Sci. Soc. Am. J. 44: 1216–1221.
Paltineanu, I.C., and J.L. Starr. 1997. Real-time soil water dynamics using multisensor capacitance probes: Laboratory calibration. Soil Sci. Soc. Am. J. 61:1576–1585.
Parkhurst, D.L., and C.A.J. Appelo. 1999. User's guide to PHREEQC (version 2)—A computer program for speciation, batch-reaction, one-dimensional transport, and inverse geochemical calculations. Water-Resources Investigation Rep. 99–4259. USGS, Denver, CO.
Rhoades, J.D., P.A.C. Raats, and R.J. Prather. 1976. Effects of liquid-phase electrical conductivity, water content, and surface conductivity on bulk soil electrical conductivity. Soil Sci. Soc. Am. J. 40: 651–655.
Robinson, D.A. 2001. Comments on "Field calibration of a capacitance water content probe in fine sand soils." Soil Sci. Soc. Am. J. 65:1570–1571.
Robinson, D.A., C.M.K. Gardner, J. Evans, J.D. Cooper, M.G. Hodnett, and J.P. Bell. 1998. The dielectric calibration of capacitance probes for soil hydrology using an oscillation frequency response model. Hydrol. Earth Sys. Sci. 2:111–120.
Roth, K., R. Schulin, H. Flühler, and W. Attinger. 1990. Calibration of time domain reflectometry for water content measurement using a composite dielectric approach. Water Resour. Res. 26:2267–2273.
Shainberg, I., and W.D. Kemper. 1966. Conductance of adsorbed alkali cations in aqueous and alcoholic bentonite pastes. Soil Sci. Soc. Am. J. 30:700–706.
Shainberg, I., and R. Levy. 1975. Electrical conductivity of Na-Montmorillonite suspensions. Clays Clay Miner. 23:205–210.
Shainberg, I., J.D. Rhoades, and R.J. Prather. 1980. Effect of exchangeable sodium percentage, cation exchange capacity, and soil solution concentration on soil electrical conductivity. Soil Sci. Soc. Am. J. 44:469–473.
Shainberg, I., J.D. Oster, and J.D. Wood. 1982. Electrical conductivity of Na/Ca-Montmorillonite gels. Clays Clay Miner. 30:55–62.
Sihvola, A. 1999. Electromagnetic mixing formulas and applications. IEE Electromagnetic Waves Series No. 47. Inst. of Electrical Eng., Stevenage, UK.
Soil Survey Staff. 2003. National Soil Survey Characterization Data. Soil Survey Laboratory, National Soil Survey Center, USDA-NRCS, Lincoln, NE.
Topp, G.C., J.L. Davis, and A.P. Annan. 1980. Electromagnetic determination of soil water content: Measurements in coaxial transmission lines. Water Resour. Res. 16:574–582.
Topp, G.C., M. Yanuka, W.D. Zebchuk, and S. Zegelin. 1988. Determination of electrical conductivity using time domain reflectometry: Soil and water experiments in coaxial lines. Water Resour. Res. 24:945–952.
Von Hippel, A.R. 1954. Dielectric materials and applications. John Wiley & Sons.
Weast, R.C. (ed.) 1985. Handbook of chemistry and physics. 65th ed. CRC Press, Boca Raton, FL.